Smart Q-switching for single-pulse generation in an erbium-doped fiber laser

Luis Escalante-Zarate,[1] Yuri O. Barmenkov,[1,*] Stanislav A. Kolpakov,[2] José L. Cruz,[3] and Miguel V. Andrés[3]

[1]*Centro de Investigaciones en Óptica, A.C., Loma del Bosque 115, Lomas del Campestre, 37150 Leon, Gto., Mexico*
[2]*Departamento de Óptica, Universidad de Valencia, Dr. Moliner 50, 46100, Burjassot (Valencia), Spain*
[3]*Departamento de Física Aplicada – ICMUV, Universidad de Valencia, Dr. Moliner 50, 46100, Burjassot (Valencia), Spain*
[*]*yuri@cio.mx*

Abstract: In this paper, we report an active Q-switching of an erbium-doped fiber laser with special modulation functions and novel laser geometry. We experimentally demonstrate that using such a smart Q-switch approach, Q-switch ripple-free pulses with Gaussian-like shape and 17.3 ns width can be easily obtained. The idea behind the smart Q-switch is to suppress one of two laser waves contra-propagating along the fiber cavity, which arises after Q-cell opening, and to eliminate the minor sub-pulses.

OCIS codes: (140.3500) Lasers, erbium; (140.3510) Lasers, fiber; (140.3540) Lasers, Q-switched.

References and links

1. J. Cascante-Vindas, A. Díez, J. L. Cruz, and M. V. Andrés, "Supercontinuum Q-switched Yb fiber laser using an intracavity microstructured fiber," Opt. Lett. **34**(23), 3628–3630 (2009).
2. W. Shi, M. A. Leigh, J. Zong, Z. Yao, D. T. Nguyen, A. Chavez-Pirson, and N. Peyghambarian, "High-power all-fiber-based narrow-linewidth single-mode fiber laser pulses in the C-band and frequency conversion to THz generation," IEEE J. Sel. Top. Quantum Electron. **15**(2), 377–384 (2009).
3. C. Cuadrado-Laborde, P. Pérez-Millán, M. V. Andrés, A. Díez, J. L. Cruz, and Y. O. Barmenkov, "Transform-limited pulses generated by an actively Q-switched distributed fiber laser," Opt. Lett. **33**(22), 2590–2592 (2008).
4. S. Adachi and Y. Koyamada, "Analysis and design of Q-switched erbium-doped fiber lasers and their application to OTDR," J. Lightwave Technol. **20**(8), 1506–1511 (2002).
5. R. J. De Young and N. P. Barnes, "Profiling atmospheric water vapor using a fiber laser lidar system," Appl. Opt. **49**(4), 562–567 (2010).
6. D. J. Richardson, J. Nilsson, and W. A. Clarkson, "High power fiber lasers: current status and future perspectives [Invited]," J. Opt. Soc. Am. B **27**(11), B63–B92 (2010).
7. S. A. Kolpakov, Y. O. Barmenkov, A. D. Guzman-Chavez, A. V. Kir'yanov, J. L. Cruz, A. Díez, and M. V. Andrés, "Distributed Model for Actively Q-Switched Erbium-Doped Fiber Lasers," IEEE J. Quantum Electron. **47**(7), 928–934 (2011).
8. Y. Wang and C.-Q. Xu, "Switching-induced perturbation and influence on actively Q-switched fiber lasers," IEEE J. Quantum Electron. **40**(11), 1583–1596 (2004).
9. A. Othonos and K. Kalli, *Fiber Bragg Gratings: Fundamentals and Applications in Telecommunications and Sensing* (Artech House, 1999), Chap. 2.
10. M. J. F. Digonnet, ed., *Rare-earth-doped fiber lasers and amplifiers*, 2nd ed. (Marcel Dekker, 2001, p. 568).
11. V. Gapontsev, V. Fomin, A. Ount, and I. Samartsev, "100 kW ytterbium fiber laser," Proc. SPIE **3613**, 49–54 (1999).
12. R. Xin and J. D. Zuegel, "Amplifying nanosecond optical pulses at 1053 nm with an all-fiber regenerative amplifier," Opt. Lett. **36**(14), 2605–2607 (2011).

1. Introduction

Actively Q-switched fiber lasers (QS-FLs), particularly those operate in the eye-save optical range, have attracted increasing attention in various practical fields, such as fundamental science, super-continuum generation [1], nonlinear frequency conversion [2], distributed fiber-optical sensing [3], optical time-domain reflectometry [4], light detection and ranging (LIDAR) [5], etc.

Active Q-switching (QS) is usually achieved in fiber lasers (FLs) using bulk acousto-optic modulators (AOMs) that modulate rapidly the intra-cavity loss (a standard AOM rise-time is

#158338 - $15.00 USD Received 28 Nov 2011; revised 20 Jan 2012; accepted 26 Jan 2012; published 8 Feb 2012

of the order 10 – 100 ns), which allows the generation of QS-pulses with widths from approximately ten to a few hundred of nanoseconds [6].

Recently, it has been shown that when the FL cavity round-trip time is longer than the AOM rise-time, the Q-switch pulses are composed of a number of sub-pulses that are separated by an interval approximately equal to the cavity round-trip time. This multi-peak shape of Q-switch pulses is attributed to spatial-temporal oscillations in power of the laser wave that travels through the FL cavity and depopulates the laser level of the active ions non-uniformly along the active fiber length [7, 8]. It was also noted that conventional Q-switching does not provide for a robust and flexible control of the output temporal pulse shape [6].

In this paper, we propose a "symmetric" QS-FL scheme in which the AOM divides the active fiber into two equal comparatively short sections. Such scheme permits one to protect the laser against spurious lasing when the AOM is blocked and therefore to growth the population inversion resulting in the Q-switch pulse energy increase. The total lengths of the FL cavity sections located on both sides of the AOM, as well as the AOM switching function, were chosen so that single narrow QS pulses were produced at the AOM repetition frequency. We demonstrate that free-ripple QS pulses with Gaussian-like shape and 17 ns in width can be easily obtained in our experimental conditions when a special modulation function is applied.

This technique that combines a specific cavity design with a special Q-factor modulation function is what we call "smart Q-switch". The results of using this technique differs dramatically from those obtained using a simple one-step switching function.

2. Experimental setup

A schematic of the QS-FL is shown in Fig. 1. The laser cavity consists of two pieces of a standard low-doped erbium fiber (EDF) (*Thorlabs*, M5-980-125, low-power absorption at 979 nm is about 5 dB/m) located on both AOM sides (EDF1 and EDF2).

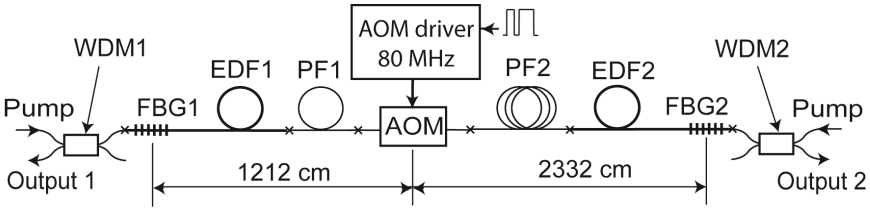

Fig. 1. Schematic diagram of QS-FL. Crosses indicate the fiber splices.

The EDFs' lengths were chosen not to be too long, of about 4 m, which helps to suppress spurious lasing when the AOM is closed. Otherwise, when EDF length on each AOM side is higher than 4 m, spurious lasing observed due to weak back-reflection from the closed AOM decreases the population inversion and therefore reduces the QS pulse energy. Two fiber Bragg gratings (FBG1 and FBG2) are the FL cavity couplers. The reflectivity of FBG1 is 93%, and that of FBG2 is 33%; their spectra are mechanically tuned to 1552 nm. The bandwidth of FBGs is around 100 pm.

To decrease the intra-cavity loss, the FBGs were recorded directly in the EDF pieces after preliminary hydrogenation [9]. The total cavity length was 35.44 m (see Fig. 1). Such a comparatively long FL cavity was chosen in order to control the shape of the QS pulses (see below).

The fiber coupled AOM (Gooch & Housego, M111-2J-F2S) operates at a wavelength of 1550 nm with a driving acoustical frequency of 80 MHz. The AOM rise-time is 50 ns (see Fig. 2); its transmission in the open state is 38% and the extinction ratio is better than 50 dB. In order to increase the FL cavity length, two pieces of the passive fiber (PF1 and PF2) were placed between the AOM and the EDFs.

#158338 - $15.00 USD Received 28 Nov 2011; revised 20 Jan 2012; accepted 26 Jan 2012; published 8 Feb 2012

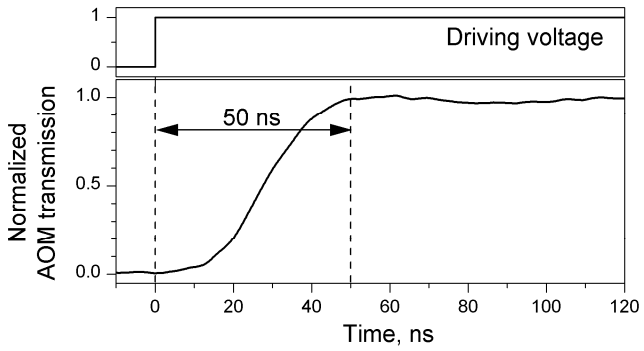

Fig. 2. AOM switching process. The upper graph shows the signal applied to the AOM driver.

The laser was pumped through 980/1550 nm wavelength-division multiplexers (WDM1 and WDM2) with commercial fiber-coupled semiconductor lasers operated at 976 nm.

3. Experimental results and discussion

Figure 3 shows typical QS pulses emitted at 1552 nm from the laser pumped with 200 mW from both sides; the repetition rate was 200 Hz. It is seen that the shape of the pulses strongly depends on the control signal applied to the AOM driver. The pulse depicted in Fig. 3(a) corresponds to "classical" QS when the AOM is opened rapidly with the step function shown in Fig. 2 (the signal applied to the AOM driver is shown in the inset). The overall QS pulse consists of several sub-pulses; the interval between the sub-pulses 1a and 1b, 1b and 1c, and also between 2a and 2b, and 2b and 2c, corresponds to the cavity round-trip time (≈340 ns). Thus, two groups of sub-pulses are observed, each group belongs to one of two contra-propagating laser waves arising at the moment when the AOM switches on.

The sub-pulses plotted with blue color (left scale) have very low power; actually they are the seed of the strong QS-pulses, which are registered just after the AOM switching on. The first sub-pulse (1a) belongs to the wave that starts traveling along the cavity to the right direction (wave-1) (see Fig. 4). This sub-pulse consists of the amplified spontaneous emission (ASE) born in EDF1 and then amplified in EDF2. The largest part of power of this sub-pulse is lost on propagating through FBG2, due to the relatively narrow spectral band reflected by the FBG. Thus, the signal that is reflected by FBG2 takes a very small part (~10^{-3}) of the whole sub-pulse power. After propagating along the cavity for one round-trip more, this pulse is amplified enough to be visible (see sub-pulse 1b, right scale in Fig. 3).

The sub-pulse 2a belongs to another laser wave (wave-2), which starts to travel along the cavity in the opposite direction with respect the direction of wave-1 and cover 1.5 one-way trips along the cavity. After covering one round-trip more, this sub-pulse leaves the cavity as the sub-pulse 2b. Since this sub-pulse travels along 16 m of EDF more than sub-pulse 1b, it is amplified to a power value that is much higher than that of the sub-pulse 1b.

The sub-pulses 1c and 2c travel through the cavity for 4.5 and 5.5 one-way trips, respectively. For these two sub-pulses, the EDF is already "discharged", which results in low power sub-pulses with decreased amplitudes. All the other sub-pulses that travel along the cavity for 6.5, 7.5 and more times are too small to be detectable.

As seen in Fig. 1, the FL geometry is not completely symmetric. The left arm of the cavity is approximately two times shorter than the right arm. Such laser asymmetry was chosen specifically to suppress one of two contra-propagating laser waves at the beginning of QS pulse formation. Figure 3(b) shows an example of the QS pulse, in which sub-pulse 1b does not exist. This situation was achieved by using a two-step AOM opening (see inset in Fig. 3(b)): during the first AOM on/off cycle, wave-2 passes through the AOM to the left direction; then it is reflected by FBG1 and passes through the AOM for the second time, to the right direction. At the same time, wave-1 also passes through the AOM (to the right

#158338 - $15.00 USD Received 28 Nov 2011; revised 20 Jan 2012; accepted 26 Jan 2012; published 8 Feb 2012

direction) and then it is reflected by FBG2. (Note that at the moment of reflection by FBG2, ASE with the optical spectrum lying outside the FBG2 reflection band, forms the sub-pulse 1a, see the blue curve in Fig. 3(b)). Finally, when wave-1 approaches the AOM for the second time, the latter is completely closed, thereby stopping propagation of this wave. Thus, only one laser wave (wave-2 in our case) travels through the cavity.

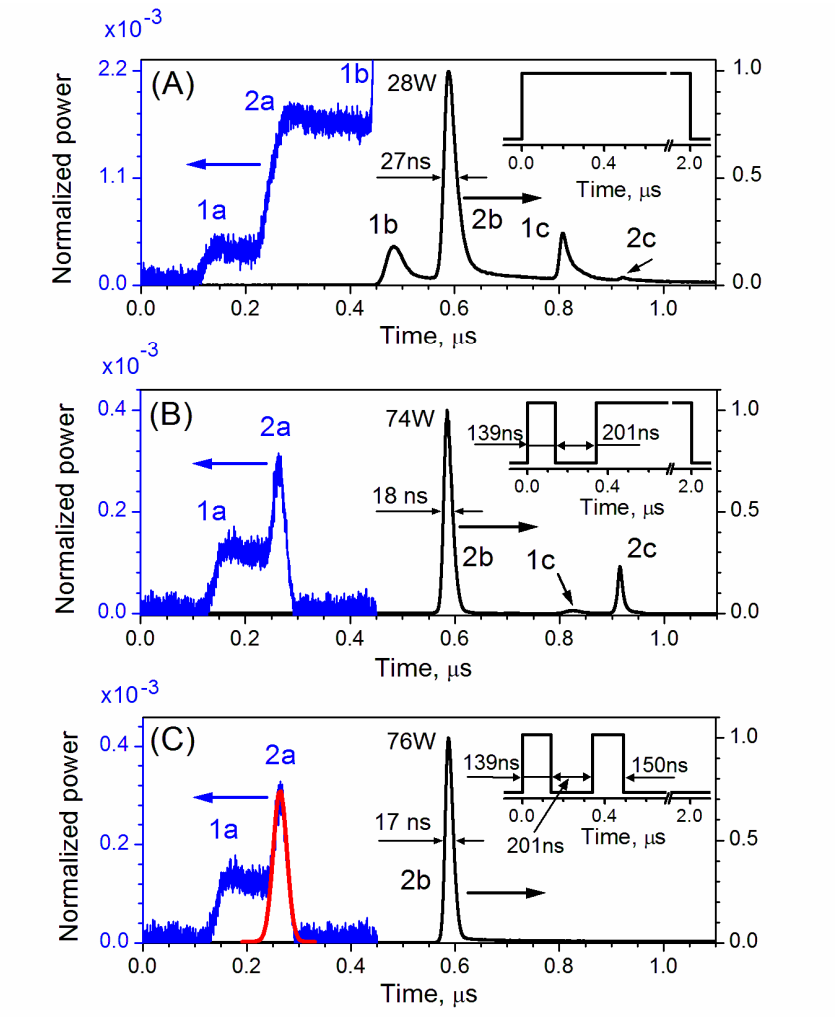

Fig. 3. Experimental QS-pulses normalized to peak power of sub-pulse 2b. The insets show the shapes of the signal applied to the AOM driver. All pulses were measured from the right laser output (Output 2, see Fig. 1). The values of peak power of some sub-pulses are indicated.

#158338 - $15.00 USD Received 28 Nov 2011; revised 20 Jan 2012; accepted 26 Jan 2012; published 8 Feb 2012

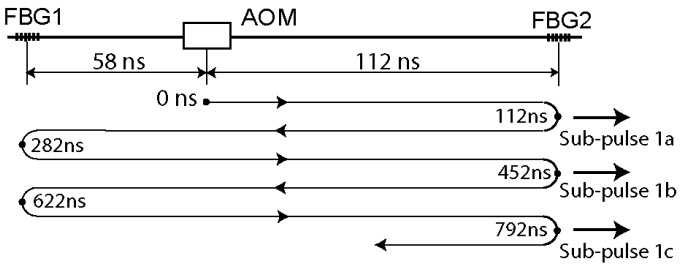

Fig. 4. Diagram showing how the wave-1 travels through the cavity. Due to the delay introduced by the AOM, the pulses' maxima (see Fig. 3(a)) are slightly delayed with respect to the moments indicated in the diagram.

As seen in Fig. 3(b), the AOM forms the narrow sub-pulse 2a by cutting out the laser signal with its switching off edge at 139 ns; this sub-pulse is approximated well with a Gaussian function (the residual sum is $R^2 = 0.983$) with FWHM of 26 ns (the red curve in Fig. 3(c)). The small sub-pulse 1c corresponds to the wave-1 arising after the second opening of the AOM. To suppress this sub-pulse and the last sub-pulse 2c, the AOM should be quickly closed after the second step of AOM opening.

Figure 3(c) shows the QS pulse emitted by the laser when the AOM is switched on in two short steps (see inset), thereby suppressing the sub-pulses 1b, 1c and 2c. (The sub-pulse 2b shown in Fig. 3(c) is actually the sub-pulse 2b depicted also in Figs. 3(a) and 3(b)). It is seen that in this case the QS-pulse is shortest (FWHM is 17.3 ns). In fact, this sub-pulse is the most powerful in the series of Figs. 3(a), 3(b) and 3(c). The effect of pulse narrowing (compare the sub-pulse 2b with sub-pulse shown by the red curve) is explained by a strong amplification of the pulse's leading edge by a still "charged" EDF and by the absorption of its trailing edge by a partially "discharged" EDF. This effect has been observed in saturated fiber amplifiers [10, 11].

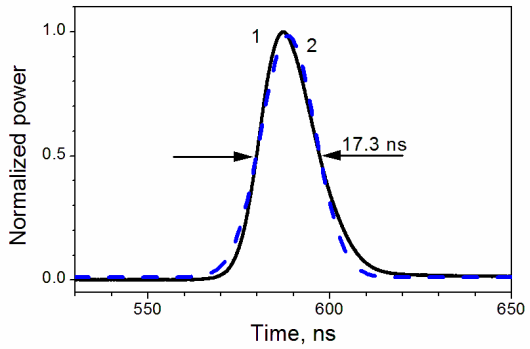

Fig. 5. Gaussian-like shape of the QS pulse emitted when the AOM is opened in two short steps. Curve 1 (solid line) corresponds to the experimental pulse and curve 2 (dashed line) to the best fit. The residual sum $R^2 = 0.989$.

The operation principle of the two-step QS-FL is quite similar to that of a multi-pass optical amplifier [12]; the difference is that in our case the seed pulse is formed inside the FL cavity by the AOM. The shape of the QS pulse shown in Fig. 3(c) is Gaussian-like (see Fig. 5); the peak power of this pulse differs by 35 dB with respect to peak power of the seed pulse (sub-pulse 2a in Fig. 3(c)). The energy of the pulse 2b (Figs. 3(b) and 3(c)) is 1.1 μJ, whereas the energy of the QS pulses (including all sub-pulses) depicted in Fig. 3(a) and (b) is around 1.6 – 1.7 μJ. The ASE power measured when the AOM was switched off for long time is around 0.8 mW. Thus, the signal-to-noise ratio measured as a ratio of the pulse peak power to the ASE power is ≈50 dB.

#158338 - $15.00 USD Received 28 Nov 2011; revised 20 Jan 2012; accepted 26 Jan 2012; published 8 Feb 2012

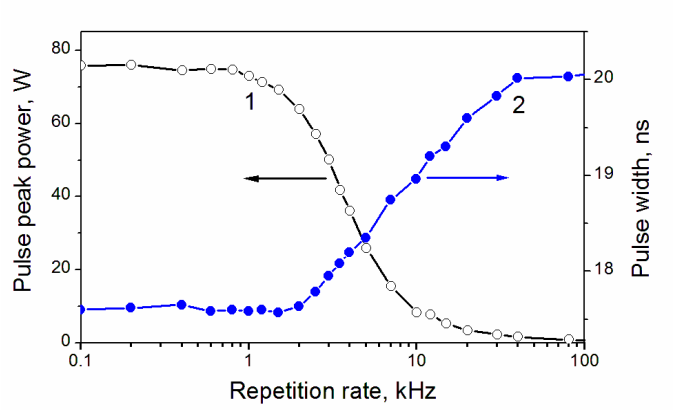

Fig. 6. Peak pulse power (curve 1) and pulse width (curve 2) as a function of repetition rate of two-step Q-switch driven by the signal shown in the inset to Fig. 3(c).

The laser was operated at various repetition rates, always upon AOM two-short-step opening as shown in Fig. 3(c). Figure 6 shows dependencies of pulse peak power and pulse width on QS repetition rate in the range 100 Hz – 100 kHz. The laser was pumped with 200 mW from both sides. As it was expected, QS pulses become stronger and shorter as repetition rate decreases; when repetition rate is higher than 1 kHz, the pulse power decreases drastically, whereas the pulse width is always within the interval from ≈17 ns at a low repetition rate to ≈20 ns at a high repetition rate. The latter feature may be explained by the fact that the AOM two-step switching shapes the seed QS sub-pulse by suppressing its trailing edge (see Fig. 3(c)), with further shortening by saturated EDF amplification.

4. Conclusion

We have reported the improvements that can be achieved in Q-switched erbium-doped fiber lasers by using novel laser geometry and a special modulation function of a Q-switch cell (in our case we used two-short-step Q-switching). We have experimentally demonstrated that such a smart Q-switch permits the formation of single QS pulses without any ripples. Using an AOM with a rise-time of 50 ns, short QS pulses with FWHM of 17 ns and peak power of 76 W were obtained. The parameters of QS pulses may be improved by optimizing the intra-cavity elements, including EDF concentration and length, AOM rise-time, FBGs' reflections, etc. Using an AOM with a short rise-time can help to decrease the FL cavity length and to shorten the Q-switch pulses.

The proposed QS-FL may be used as a master oscillator for further amplifying in MOPA [6]. Furthermore, the idea of smart Q-switching may be applied to powerful Yb-doped or Er/Yb-codoped Q-switched fiber lasers for the generation of ripple-free narrow pulses.

Acknowledgments

This work was supported in part by the Ministerio de Educación y Ciencia (Project TEC2008-05490), by the Generalitat Valenciana (Project PROMETEO/2009/077), and by the Ministerio de Educación (Ref. SAB2009-0061), all from Spain.

#158338 - $15.00 USD Received 28 Nov 2011; revised 20 Jan 2012; accepted 26 Jan 2012; published 8 Feb 2012